

Enhanced band-gap luminescence in strain-symmetrized $(\text{Si})_m/(\text{Ge})_n$ superlattices

U. Menczigar and G. Abstreiter

Walter-Schottky-Institut, Technische Universität München, Am Coulombwall, D-8046 Garching, Germany

J. Olajos and H. Grimmeiss

Department of Solid State Physics, University of Lund, Box 118, S-221 00 Lund, Sweden

H. Kibbel, H. Presting, and E. Kasper

Daimler Benz AG, Forschungszentrum, Wilhelm Runge Strasse 11, D-7800 Ulm, Germany

(Received 18 September 1992; revised manuscript received 25 November 1992)

We report on band-gap luminescence in strain-symmetrized, $(\text{Si})_m/(\text{Ge})_n$ superlattices grown on a step-graded, alloy buffer with a reduced dislocation density, using Sb as a surfactant. The luminescence efficiency for a $(\text{Si})_9/(\text{Ge})_6$ and $(\text{Si})_6/(\text{Ge})_4$ superlattice is strongly enhanced compared with a corresponding $\text{Si}_{0.6}\text{Ge}_{0.4}$ alloy reference sample. The luminescence signals can be attributed to interband transitions of excitons localized at potential fluctuations in the superlattice. The observed systematic shift of the band-gap luminescence to lower energies with increasing period length compares well with results of a simple, effective-mass calculation. An increasing superlattice band gap and a reduction in luminescence intensity is observed if the Si and Ge layers are interdiffused by thermal annealing. The band gap for a $(\text{Si})_6/(\text{Ge})_4$ superlattice was also measured with absorption spectroscopy. The absorption coefficient, as determined by direct transmission, is in the order of 10^3 cm^{-1} about 0.1 eV above the band gap.

$(\text{Si})_m/(\text{Ge})_n$ strained-layer superlattices (SLS's) have attracted considerable attention because of their capacity to function as efficient Si-based, light-emitting semiconductors in the near-infrared region. An enhanced luminescence efficiency for $(\text{Si})_m/(\text{Ge})_n$ SLS's, compared with the indirect semiconductors Si and Ge, was predicted already 18 years ago.¹ Due to the progress in the optimization of Si molecular-beam epitaxy (MBE), SLS's with atomically sharp interfaces could be realized on different substrates.²⁻⁴ The first observations of interband transitions in a $(\text{Si})_4/(\text{Ge})_4$ SLS quantum well⁵ stimulated a large number of band-structure calculations.^{6,7} As shown by the majority of these theoretical investigations, SLS's with a "quasidirect," fundamental band gap are expected only if the Si layers are under a tensile lateral strain. This requires the growth of $(\text{Si})_m/(\text{Ge})_n$ SLS's on relaxed, $\text{Si}_{1-x}\text{Ge}_x$ alloy, buffer layers. Photoluminescence (PL) studies by Zachai *et al.*⁸ on SLS's grown on partly relaxed buffer layers showed indeed strong luminescence in the infrared region. Their results, however, proved to be controversial, as witnessed by the discussions they provoked⁹ because of the fact that a high dislocation density of about 10^{10} cm^{-2} was present in the samples. Only very recently could the band gap of strain-symmetrized $(\text{Si})_n/(\text{Ge})_n$ SLS's ($n=4,5,6$) be measured using PL, electroluminescence, and absorption spectroscopy.^{10,11} The major goal for the achievement of greater efficiency of light emission by the $(\text{Si})_m/(\text{Ge})_n$ SLS is the reduction of the dislocation density imposed by the relaxed alloy, buffer layer. A reduction of the dislocation density by several orders of magnitude was recently demonstrated by growing completely relaxed alloys with a linear¹² or step-graded^{13,14} Ge concentration profile on Si(100). The PL efficiency of $\text{Si}_{1-x}\text{Ge}_x$ alloys was also improved considerably at growth temperatures above 500°C.¹⁵ In addition it has been shown that

$(\text{Si})_m/(\text{Ge})_n$ SLS's with sharp interfaces can be produced at these high temperatures using surfactant techniques.^{14,16,17} Based on these developments we are able to achieve an enormous improvement in the quality of strain-symmetrized $(\text{Si})_m/(\text{Ge})_n$ SLS's. Here we report on strongly enhanced band-gap PL in $(\text{Si})_6/(\text{Ge})_4$ and $(\text{Si})_9/(\text{Ge})_6$ SLS's grown on step-graded $\text{Si}_{1-x}\text{Ge}_x$ alloy buffers. The results clearly support the earlier results using samples of lower quality,^{8,10,11} and are in contradiction to the theoretical work of Ref. 9.

The $(\text{Si})_9/(\text{Ge})_6$, $(\text{Si})_6/(\text{Ge})_4$, $(\text{Si})_3/(\text{Ge})_2$ SLS's and the $\text{Si}_{0.6}\text{Ge}_{0.4}$ alloy buffer reference sample were grown in a home-made Si-MBE chamber.¹⁴ The buffer layer consists of a step-graded alloy buffer with a thickness of 6500 Å, followed by a 5000-Å-thick $\text{Si}_{0.6}\text{Ge}_{0.4}$ alloy. In the step-graded region of the buffer the Ge content was increased stepwise by 3%/500 Å, while the temperature was continuously lowered from 600°C down to 520°C. The residual lateral strain in the topmost $\text{Si}_{0.6}\text{Ge}_{0.4}$ alloy was determined by x-ray diffraction (XRD) to be -0.03% . The SLS's with an entire thickness of 2000 Å [$(\text{Si})_3/(\text{Ge})_2$], 1500 Å [$(\text{Si})_6/(\text{Ge})_4$], and 3000 Å [$(\text{Si})_9/(\text{Ge})_6$] were deposited on top of the alloy buffer at $T=500^\circ\text{C}$. Prior to the growth of the SLS's, a monolayer (ML) of Sb was deposited to act as a surfactant. The $(\text{Si})_6/(\text{Ge})_4$ SLS was characterized in detail with XRD, transmission electron microscopy (TEM),¹⁸ and Raman scattering. The dislocation density, measured with cross-sectional TEM, was found to be reduced by two orders of magnitude compared with previously studied $(\text{Si})_m/(\text{Ge})_n$ SLS's (Refs. 8, 10, and 11) grown on partly relaxed alloy buffer layers. The period length is 15.5 ± 0.5 Å. The average Ge concentration, as determined by energy-dispersive XRD, is 45%. The lateral lattice constant is 5.499 Å, which results in an average la-

teral strain in the SLS of -0.3% . The deviations for all samples from their nominal structural data are less than 10%.

The PL was excited by the 457-nm line of an Ar⁺ laser. The excitation power density varied between ~ 0.05 and 50 mW/mm^2 . The samples were mounted in a variable temperature, He cryostat. PL signals were analyzed with a 64-cm grating monochromator and detected by either a Ge or an InAs detector, in both cases cooled by liquid nitrogen. The absorption was measured by means of parallel photoconductivity (PC). The direct transmission (DT) was measured using an external, liquid-nitrogen-cooled InSb photodetector. The DT and PC measurements were performed at $T=10 \text{ K}$ on a Bomem DA3.02, Fourier transform, infrared spectrometer. Annealing was performed in a quartz furnace under vacuum conditions ($p < 10^{-6} \text{ mbar}$).

The PL spectra for all samples are shown in Fig. 1. The random-alloy sample shows two peaks at 0.985 and 0.929 eV which can be attributed to a no-phonon (NP) transition and an associated phonon replica involving a transverse-optical Si-Si mode ($\text{TO}^{\text{Si-Si}}$), respectively.¹⁹ These transitions originate in the 5000-Å-thick $\text{Si}_{0.6}\text{Ge}_{0.4}$ alloy. The calculated band-gap energy of 0.988 eV, taking into account the residual, built-in strain, compares well with the energy position of the NP line. For the $(\text{Si})_3/(\text{Ge})_2$ SLS the PL signals detected at 0.984 and 0.928 eV can also be attributed to a NP transition and a $\text{TO}^{\text{Si-Si}}$ replica. The PL intensity is enhanced by a factor of 5 compared with the alloy. The longer-period SLS's show much stronger PL signals at 0.877, 0.825, 0.778, and 0.726 eV, respectively. As shown below, these PL signals can be attributed to a NP transition of localized excitons (LE^{NP}) and an associated phonon replica (LE^{TO}). Taking into account the fact that the thickness of the SLS region is much smaller than the thickness of the $\text{Si}_{0.6}\text{Ge}_{0.4}$ alloy layer, the intensity of the LE^{NP} line is enhanced by about a factor of 150 [$(\text{Si})_6/(\text{Ge})_4$] and 90

[$(\text{Si})_9/(\text{Ge})_6$]. The enhanced PL intensity for $(\text{Si})_6/(\text{Ge})_4$ compared with $(\text{Si})_9/(\text{Ge})_6$ is in qualitative agreement with calculations of the oscillator strength for these SLS's.⁶ The energy positions of the NP lines as a function of the period length are shown in the inset of Fig. 1 and are compared with the results of an effective-mass (EM) calculation^{8,20} for strain-symmetrized $(\text{Si})_m/(\text{Ge})_n$ SLS's ($m/n = \frac{3}{2}$). The calculated band gaps are determined by the energy difference between the twofold-degenerate $\Delta(2)$ minima in the conduction band (CB) and light-hole (lh) [heavy-hole (hh)] states in the valence band (VB). In this calculation, the Si concentration (x_{Si}) in the Si layers of the SLS's is assumed to be reduced with decreasing Si layer thickness (d_{Si}) due to the intermixing of the Si and Ge layers during growth at $T=500^\circ\text{C}$. x_{Si} is assumed to depend on d_{Si} as

$$x_{\text{Si}} = 1 - 0.4 / [1 + \exp(d_{\text{Si}} - 4.0 \text{ \AA}) / 1.0 \text{ \AA}]. \quad (1)$$

The effective masses, deformation potentials (DP), and band offsets used in this calculation are those given in Ref. 8. For the alloy, values that were linearly interpolated between those of Si and Ge were used. The energy positions of the NP lines for the alloy and the $(\text{Si})_3/(\text{Ge})_2$ SLS are almost identical, which indicates that the $(\text{Si})_3/(\text{Ge})_2$ SLS is more like an alloy due to the intermixing. The systematic shift of the NP lines for $(\text{Si})_6/(\text{Ge})_4$ and $(\text{Si})_9/(\text{Ge})_6$ to lower energies with increasing period length is well described by the calculation. Deviations for the SLS's from the nominal structural data result in slightly different calculated band-gap energies. These deviations, however, are of the same order of magnitude as the theoretical errors arising from the uncertainties in deformation potentials given in the literature.

In order to identify the nature of the LE^{NP} and LE^{TO} lines, the $(\text{Si})_6/(\text{Ge})_4$ SLS was subsequently annealed at temperatures of 600, 650, and 780°C for 1 h. After the first annealing step at 600°C [Fig. 2(b)], both the LE^{NP} and LE^{TO} line are shifted to higher energies compared to the as-grown sample [Fig. 2(a)] while the intensities are reduced. Broad PL bands appear in the spectrum below the energy position of the LE^{TO} line, which may be attributed to defect-related transitions. Subsequent annealing of the sample at 650°C results in a further upward shift of the energy position of the LE^{NP} line [Fig. 2(c)]. After a final annealing step at 780°C intense defect lines (D_1, D_2) appear in the spectrum [Fig. 2(d)] which are due to dislocations generated by the relief of the residual strain of about -0.3% .²¹ A further broad peak appears at 0.977 eV (L) which looks similar to PL signals observed by Noël *et al.* in Si/SiGe quantum-well structures after thermal annealing.²² The weak PL line observed at 1.008 eV (NP^{alloy}) is due to a NP transition in the $\text{Si}_{0.55}\text{Ge}_{0.45}$ alloy¹⁹ as the SLS, with an average Ge concentration of 45%, is finally completely interdiffused. The band gap of the SLS as a function of annealing can be modeled using the EM calculation in conjunction with an interdiffusion model of Schorer *et al.*²³ The calculated transition energies between the $\Delta(4)$ and $\Delta(2)$ minima in the CB and the lh and hh states in the VB for a strain-symmetrized SLS with a period length of 15.5 Å and an average Ge concentration of 45% are shown in the inset

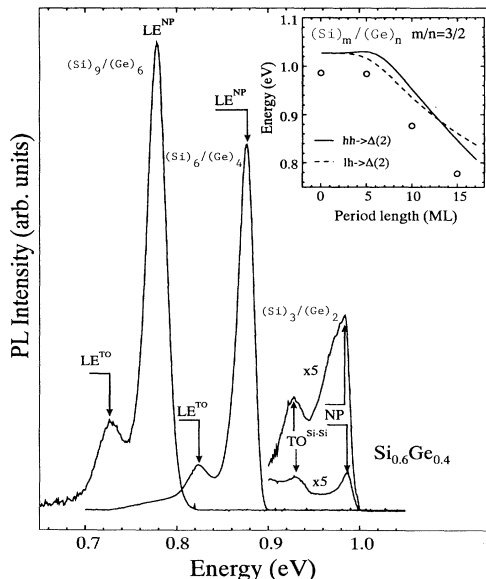


FIG. 1. PL spectra for $(\text{Si})_9/(\text{Ge})_6$, $(\text{Si})_6/(\text{Ge})_4$, $(\text{Si})_3/(\text{Ge})_2$ SLS's, and a $\text{Si}_{0.6}\text{Ge}_{0.4}$ alloy.

of Fig. 2 as a function of the Si concentration in the Ge layers. The dots mark the energy position of the LE^{NP} and NP^{alloy} line of the as-grown and completely alloyed sample, respectively. The observed systematic shift of the energy position for the LE^{NP} line to higher energies with an increasing degree of interdiffusion is in qualitative agreement with the calculated band gaps. The energy difference between LE^{NP} and LE^{TO} , which is 52 meV for both $(Si)_6/(Ge)_4$ and $(Si)_9/(Ge)_6$, does not change with interdiffusion. This gives clear evidence that also the LE^{TO} line can be assigned to transitions between lh and $\Delta(2)$ states across the SLS band gap. The energy difference between the LE^{NP} and LE^{TO} line of 52 meV compares very well with the energy of Si-Ge optical phonons measured with Raman scattering. The LE^{TO} signal could therefore be attributed to a phonon replica due to local Si-Ge modes at the Si/Ge interface.

Band-structure calculations undertaken by Turton and Jaros predict a reduced transition probability with increasing intermixing of the Si and Ge layers.⁶ This is reflected in the decreasing intensity of the LE^{NP} and LE^{TO} lines with an increasing degree of interdiffusion.

PL spectra for the $(Si)_6/(Ge)_4$ SLS at different temperatures are shown in Fig. 3. The intensity of both LE^{NP} and LE^{TO} lines decreases strongly with increasing temperature. At $T=29$ K only PL signals related to defects are observed whose line shapes and energy positions are very similar to such PL signals observed for the alloy sample below 0.9 eV (Fig. 4). The peak energy of the LE^{NP} and LE^{TO} line decreases linearly with increasing temperature by 0.77 meV/K. The inset in Fig. 3 shows

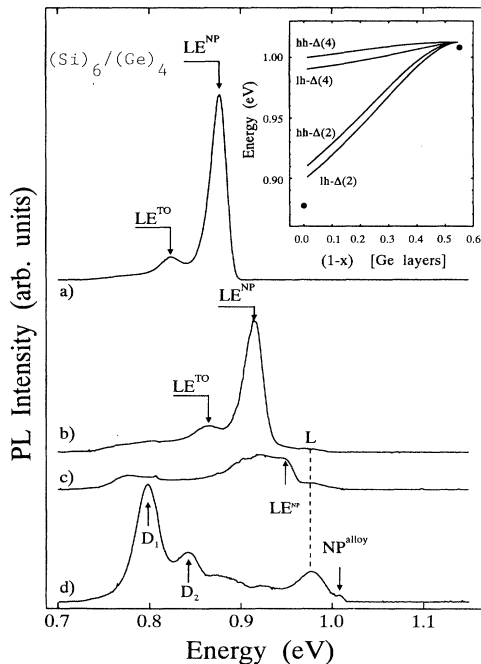


FIG. 2. PL spectra for a $(Si)_6/(Ge)_4$ SLS. Spectrum (a) for the as-grown sample, spectrum (b), (c), and (d) after subsequent annealing for 1 h at 600, 650, and 780 °C, respectively. The inset shows results of an EM calculation. Dots mark the positions of the NP line for spectrum (a) and (d).

PL spectra measured with different excitation power densities (P_{ex}). The maximum is shifted to higher energies with increasing P_{ex} . The intensity (I) versus P_{ex} is given by $I \propto (P_{ex})^{0.63}$ at $T=5$ K. The intensity on the low-energy side of the LE^{NP} line is well described by $I \propto \exp(E/E_0)$ with $E_0=10$ meV. All these findings are consistently described in terms of the recombination of excitons localized at random potential fluctuations which are expected due to slight variations in both the strain distribution and the thicknesses of the Si and Ge layers. The PL line shape for localized excitons (LE) can be written as²⁴

$$I(E, T) = \exp(E/E_0) \{ 1 + \nu \exp[-(E - E_0)/(k_B T)] \}^{-1}. \quad (2)$$

The first term describes the density of states caused by a fluctuating potential, the second term is the radiative efficiency. Carriers which are thermally excited to an energy E_C become mobile and can more easily recombine nonradiatively. ν is the radiative lifetime times an effective frequency for thermal excitation attempts. Both the observed upward shift of the PL peak position with P_{ex} and the line shape of the LE^{NP} line below the peak energy can be explained by the filling of higher states. This is also reflected in the sublinear dependence of the PL intensity on P_{ex} . Also the observed shift of the peak positions to lower energies with increasing temperature is qualitatively described by Eq. (2).²⁴

The absorption spectra of the alloy and the $(Si)_6/(Ge)_4$ SLS, measured by means of parallel photocurrent (PC), are shown in Fig. 4 together with the PL spectra. The photocurrent, after correction for the photon flux, is directly proportional to the absorption coefficient if the photon flux can be considered to be constant in the total layer. One has to take into account, however, that additional signals from the underlying alloy buffer layer are detected. The onset of absorption for the alloy compares

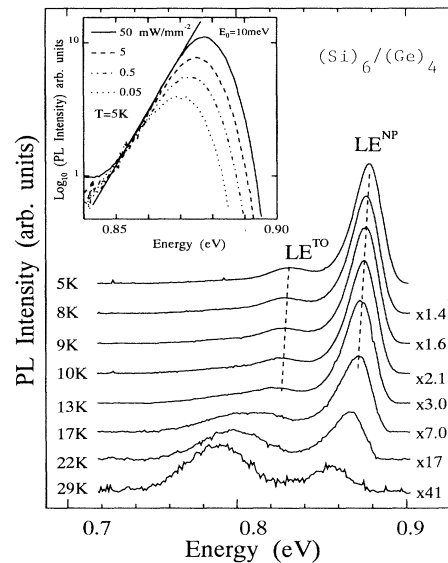


FIG. 3. PL spectra for a $(Si)_6/(Ge)_4$ SLS at different temperatures. The inset shows PL spectra at $T=5$ K taken with different excitation power densities.

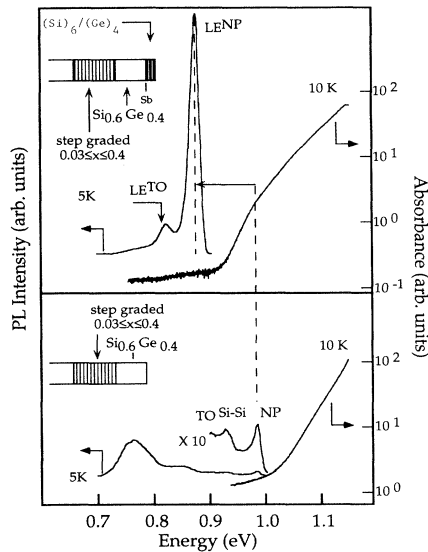


FIG. 4. PL and absorption spectra for a $(\text{Si})_6/(\text{Ge})_4$ SLS and a $\text{Si}_{0.6}\text{Ge}_{0.4}$ alloy sample.

well with both the energy position of the NP line and the calculated band-gap energy. For the SLS the onset is shifted about 100 meV to lower energies close to the energy position of the LE^{NP} line. This gives clear evidence that both the onset of absorption and the LE^{NP} line are due to transitions across the reduced SLS band gap. A weak additional kink in the absorption spectrum above 1.0 eV originates from transitions across the band gap of the underlying $\text{Si}_{0.6}\text{Ge}_{0.4}$ alloy buffer layer.

Also the total absorbance was determined in DT using

a differential method. In this experiment, the transmittance of the $(\text{Si})_6/(\text{Ge})_4$ SLS sample was measured under identical conditions as regards temperature, intensity, and angle of incidence of the IR light as the transmittance of the alloy reference sample. The absorption coefficient in the energy region of about 0.1 eV above the band gap is about $1 \times 10^3 \text{ cm}^{-1}$. It should be noted that this measured absorption coefficient is enhanced roughly by a factor of 100 compared with a corresponding $\text{Si}_{1-x}\text{Ge}_x$ alloy,²⁵ which is in agreement with the enhanced oscillator strength observed with PL.

In conclusion, we have observed enhanced band-gap PL in high-quality strain-symmetrized $(\text{Si})_m/(\text{Ge})_n$ SLS's grown on step-graded, alloy buffer layers with a drastically reduced dislocation density. The SLS band gap, which was also measured by absorption spectroscopy, is reduced compared to a corresponding alloy and can be easily modeled with an effective-mass calculation. The SLS PL can be assigned to localized excitons bound to random potential fluctuations probably caused by slight variations in the strain distribution and layer thicknesses. The SLS PL efficiency is strongly enhanced compared to the excitonic luminescence observed for the corresponding alloy. The enhanced transition probability is also reflected in an increased absorption coefficient of about 10^3 cm^{-1} .

Fruitful discussions with M. Jaros, R. Schorer, J. Engvall, and L. Samuelsson are gratefully acknowledged. This work was partially financed by the European Basic Research programme (ESPRIT) under Contract No. P7128 and by the Bank of Sweden Tercentenary foundation.

- ¹U. Gnuzmann and K. Clausecker, *Appl. Phys.* **3**, 9 (1974).
- ²J. Bevk, A. Ourmazd, L. C. Feldman, T. P. Pearsall, J. M. Bonar, B. A. Davidson, and J. P. Maennaerts, *Appl. Phys. Lett.* **50**, 760 (1987).
- ³K. Eberl, G. Krötz, R. Zachai, and G. Abstreiter, *J. Phys. (Paris) Colloq.* **5**, 329 (1987).
- ⁴E. Kasper, H. Kibbel, H. Jorke, H. Brugger, E. Friess, and G. Abstreiter, *Phys. Rev. B* **38**, 2599 (1988).
- ⁵T. P. Pearsall, J. Bevk, L. C. Feldman, J. M. Bonar, and J. P. Maennaerts, *Phys. Rev. Lett.* **58**, 729 (1986).
- ⁶R. J. Turton and M. Jaros, *Mater. Sci. Eng. B* **7**, 37 (1990), and references therein.
- ⁷U. Schmid, N. E. Christensen, M. Alouani, and M. Cardona, *Phys. Rev. B* **43**, 14 597 (1991).
- ⁸R. Zachai, K. Eberl, G. Abstreiter, E. Kasper, and H. Kibbel, *Phys. Rev. Lett.* **64**, 1055 (1990).
- ⁹U. Schmid, N. E. Christensen, and M. Cardona, *Phys. Rev. Lett.* **65**, 2610 (1990).
- ¹⁰J. Olajos, J. Engvall, H. G. Grimmeiss, U. Menczigar, G. Abstreiter, H. Kibbel, E. Kasper, and H. Presting, *Phys. Rev. B* **46**, 12 857 (1992).
- ¹¹J. Olajos, J. Engvall, H. G. Grimmeiss, H. Presting, H. Kibbel, and E. Kasper, *Thin Solid Films* (to be published).
- ¹²E. A. Fitzgerald, Y. H. Xie, M. L. Green, D. Brasen, A. R. Kortan, J. Michel, Y. J. Mie, and B. E. Weir, *Appl. Phys. Lett.* **59**, 811 (1991).
- ¹³F. K. Le Goues, B. S. Meyerson, and F. J. Morar, *Phys. Rev. Lett.* **66**, 2903 (1991).
- ¹⁴H. Presting and H. Kibbel, in Ref. 11.
- ¹⁵U. Menczigar, J. Brunner, E. Friess, M. Gail, G. Abstreiter, H. Kibbel, H. Presting, and E. Kasper, in Ref. 11 and references therein.
- ¹⁶K. Fujita, S. Fukatsu, H. Yaguchi, T. Igarashi, Y. Shiraki, and R. Ito, in *Silicon Molecular Beam Epitaxy*, edited by J. C. Beam, S. S. Jyer, and K. L. Wang, MRS Symposia Proceedings No. 220 (Materials Research Society, Pittsburgh, 1991), pp. 193–197.
- ¹⁷W. Dondl, W. Wegscheider, and G. Abstreiter, *J. Cryst. Growth* (to be published).
- ¹⁸W. Jäger, D. Stenkamp, P. Ehrhart, K. Leiffer, and W. Sybertz, in Ref. 11.
- ¹⁹J. Weber and M. I. Alonso, *Phys. Rev. B* **40**, 5683 (1989).
- ²⁰G. Bastard, *Wave Mechanics Applied to Semiconductor Heterostructures* (Les Editions de Physique, Paris, 1988).
- ²¹J. Weber and M. I. Alonso, in *Defect Control in Semiconductors*, edited by K. Sumino (Elsevier, Amsterdam, 1990), p. 1453.
- ²²J.-P. Noël, N. L. Rowell, D. C. Houghton, and D. D. Perovic, *Appl. Phys. Lett.* **57**, 1037 (1990).
- ²³R. Schorer, E. Friess, K. Eberl, and G. Abstreiter, *Phys. Rev. B* **44**, 1772 (1991).
- ²⁴M. Oueslati, M. Zouaghi, M. E. Pistol, L. Samuelson, H. G. Grimmeiss, and M. Balkanski, *Phys. Rev. B* **32**, 8220 (1985).
- ²⁵R. Braunstein, *Phys. Rev.* **130**, 869 (1963).